A defect in synapsis causes male sterility in a T-DNA-tagged *Arabidopsis thaliana* mutant

Brenda N. Peirson, Sarah E. Bowling and
Christopher A. Makaroff*
*Department of Chemistry, Miami University, Oxford,
OH 45056, USA*

Summary

Fluorescence microscopy was used to study meiosis in microsporocytes from wild-type *Arabidopsis thaliana* and a T-DNA-tagged meiotic mutant. Techniques for visualizing chromosomes and β-tubulin in other plant species were evaluated and modified in order to develop a method for analyzing meiosis in *A. thaliana* anthers. Like most dicots, *A. thaliana* microsporocytes undergo simultaneous cytokinesis in which both meiotic divisions are completed prior to cytokinesis. However, two unique events were observed in wild-type *A. thaliana* that have not been reported in other angiosperms: (1) polarization of the microsporocyte cytoskeleton during prophase I prior to nuclear envelope breakdown, and (2) extensive depolymerization of microtubules just prior to metaphase II. The first observation could have implications regarding a previously uncharacterized mechanism for determining the axis of the metaphase I spindle during microsporogenesis. The second observation is peculiar since microtubules are known to be involved in chromosome alignment in other species; possible explanations will be discussed. A T-DNA-tagged meiotic mutant of *A. thaliana* (*syn1*), which had previously been shown to produce abnormal microspores with variable DNA content, was also cytologically characterized. The first observable defect occurs in microsporocytes at telophase I, where some chromosomes are scattered throughout the cytoplasm, usually attached to stray microtubules. Subsequent developmental stages are affected, leading to complete male sterility. Based on similarities to synaptic mutants that have been described in other species, it is suggested that this mutant is defective in synaptonemal complex formation and/or cohesion between sister chromatids.

Introduction

Meiosis is comprised of a complex series of events that includes chromosome pairing, synaptonemal complex formation and crossing over, chromosome segregation, and cytokinesis. The complexity of events suggests that many genes are tightly regulated to ensure each successful meiotic division. Mutant studies are commonly used to dissect complex cellular processes; many genes causing various meiotic mutations have been reported in diverse organisms including yeast (Roeder, 1995), *Drosophila* (Orr-Weaver, 1995), *Caenorhabditis elegans* (Zetka and Rose, 1995), humans (Bickel and Orr-Weaver, 1996), and several higher plants (Kaul and Murthy, 1985).

Plants have been used for decades to study meiosis because of the accessibility of the male gametophyte (microsporocytes and pollen grains) and the synchronous development among sporogenous cells within an anther. Mutants exhibiting alterations in meiosis have been identified in numerous plant species including maize (Golubovskaya, 1989; Staiger and Cande, 1993), rice (Kitada et al., 1983), tomato (Moens, 1969), and *Arabidopsis thaliana* (Chaudhury et al., 1994; Dawson et al., 1993; He et al., 1996; Peirson et al., 1996). While most of these plants provide good models for meiotic studies due to the large size of their anthers and chromosomes, they represent relatively difficult systems for the molecular characterization of genes. *A. thaliana*, on the other hand, is ideal for molecular analysis (i.e. small genome, low levels of repetitive DNA, availability of T-DNA-tagged mutants, short generation time; Meyerowitz, 1989), but its small anthers and chromosomes have hindered cytological studies. A method for staining chromosomes in *A. thaliana* microsporocytes using propionic carmine has been reported (Vieira et al., 1990), but it does not provide the resolution required for detailed studies nor the ability to visualize cytoskeletal components. A reliable technique for the detailed analysis of meiosis in *A. thaliana* microsporocytes would provide a means for characterizing meiotic mutants and allow molecular and cytochemical studies to be combined, thereby greatly advancing the characterization of meiosis in flowering plants. In addition, a fluorescent staining method could be used in conjuction with future confocal microscopy studies.

As a first step in correlating meiotic mutant phenotypes to specific genes, preliminary cytochemical analyses were conducted on several T-DNA-tagged meiotic mutants of *A. thaliana* (Peirson et al., 1996). One such mutant line, 6492 (now referred to as *syn1*), was found to produce 'tetrads' with up to eight microspores; variable amounts of DNA were observed among the microspores, suggesting a possible defect in microtubule organization and/or chromosome arrangement during meiosis. *syn1* is also female-

sterile, indicating that the mutation is in a gene expressed in both male and female gametophytes.

In order to investigate the nature of the *syn1* mutation, we first used wild-type *A. thaliana* anthers to evaluate several techniques for analyzing meiosis (Brown and Lemmon, 1991; Clapham and Ostergren, 1984; Sonobe and Shibaoka, 1989; Vieira *et al.*, 1990). A modified fluorescence microscopy method was developed and used to characterize the events involved in wild-type *A. thaliana* male meiosis. Results obtained from the analysis of wild-type plants were then used as the basis for the characterization of *syn1*. The first observable defect in this mutant occurs in microsporocytes at telophase I where chromosome segregation and microtubule arrangement are irregular. Although most of the chromosomes segregate along the spindle to the two poles, some remain at the equator while others are scattered randomly throughout the cytoplasm, usually attached to stray microtubules. Possible causes and the effects of the misplaced chromosomes and microtubules will be discussed.

Results

Meiosis in wild-type *A.* thaliana *microsporocytes*

In order to describe meiosis in wild-type (WT) *A. thaliana* microsporocytes, we evaluated several methods for fluorescently staining chromosomes and β-tubulin. The best results were obtained by modifying published protocols. Briefly, inflorescences were pretreated with *m*-maleimidobenzoyl *N*-hydroxysuccinimide ester to stabilize cytoskeletal components (Sonobe and Shibaoka, 1989) and fixed with paraformaldehyde to maximize antibody penetration and antigenicity (Wick, 1993). Anthers from pre-bolting buds were squashed and the extruded cells were fluorescently labeled: chromosomes were stained with Hoechst 33258, and β-tubulin was observed using indirect immunofluorescence (anti-β-tubulin in conjuction with a fluorescein isothiocyanate (FITC)-conjugated secondary antibody). Potassium phosphate buffer was used throughout the fixation and staining procedures and adjusted to pH 8.0 in order to obtain maximal FITC emission (Nairn *et al.*, 1969).

Preliminary analysis of *A. thaliana* microsporogenesis indicated that meiosis occurs in *A. thaliana* buds when they are approximately 0.5–0.7 mm in length (Peirson

et al., 1996). Therefore, developmentally ordered buds were squashed and the extruded microsporocytes were analyzed for chromatin and β-tubulin organization. Meiotic figures were similar in appearance to those observed during microsporogenesis in other plant species, indicating adequate fixation and specific antigen detection.

Micrographs illustrating 14 meiotic events from prophase I to cytokinesis are shown in Figures 1 and 2. The order of events was established after observing more than 50 inflorescences and was based on the general pattern of chromosome condensation and β-tubulin organization. As the microsporocyte DNA begins to condense at early prophase I, brightly fluorescing microtubules (MTs) surround the nuclear envelope and extend into the cortical cytoplasm (Figure 1a,b). Additional DNA condensation is accompanied by a polarization of the microsporocyte cytoplasm: a few distinct MTs are present at opposite ends of the cell between the nuclear envelope and the cell wall (Figure 1c,d). After nuclear envelope breakdown, FITC-staining is observed throughout the entire microsporocyte and the condensed chromosomes are located near the center of the cell (Figure 1e,f). At metaphase I, short spindle fibers extend between the aligned chromosomes and the two poles (Figure 1g,h). Most of the MTs of the telophase I spindle are concentrated between the segregated chromosomes, and a few MTs can be seen radiating from each pole into the cortical cytoplasm (Figure 1i,j). At mid-telophase I, a phragmoplast-like structure is formed as the MT array extends centrifugally to the cell wall (Figure 1k). Unlike a typical phragmoplast, the formation of this MT array is not accompanied by cell-plate deposition. The centrally located MTs of the 'phragmoplast' extend between the two poles, while the peripheral MTs extend from pole to equator. At this stage, five chromosomes are visible at each pole and appear to be arranged in a ring (Figure 1l). As the 'phragmoplast' MTs depolymerize, a band of organelles appears along the equator of Hoechst-stained cells (Figure 1m,n). A distinct nucleolus is present within each membrane-enclosed nucleus. This late telophase I stage is observed less frequently than other stages, suggesting that it may be a relatively short phase in the meiotic process. Just prior to metaphase II, nuclear envelope breakdown occurs and the chromosomes are condensed and aligned; very little β-tubulin staining is observed (Figure 1o,p).

Metaphase II spindles contain a small number of MTs;

Figure 1. Fluorescence micrographs of meiosis in wild-type microsporocytes: early prophase I to pre-metaphase II.

(a, b) Early prophase I. (a) FITC. MTs surround nuclear envelope. (b) Hoechst. Early signs of DNA condensation. (c, d) Late prophase I. (c) FITC. MTs present at opposite ends of cell, between nuclear envelope and cell wall. (d) Hoechst. Partially condensed chromosomes. (e, f) Pre-metaphase I. (e) FITC. Staining is present throughout entire cell. (f) Hoechst. Tightly condensed chromosomes. (g, h) Metaphase I. (g) FITC. Short spindle fibers extend from aligned chromosomes to the two poles. (h) Hoechst. Chromosomes aligned along equator. (i, j) Early telophase I. (i) FITC. Most MTs are concentrated between the two poles; a few radiate into cortical cytoplasm. (j) Hoechst. Segregated chromosomes. (k, l) Mid-telophase I. (k) FITC. MTs between poles in phragmoplast-like configuration. (l) Hoechst. Five chromosomes in a ring at each pole. (m, n) Late telophase I. (m) FITC. A few interzonal MTs radiate from each nuclei. (n) Hoechst. Band of organelles along equator. A distinct nucleolus is present within each nucleus. (o, p) Pre-metaphase II. (o) FITC. Very little fluorescence. (p) Hoechst. Condensed and aligned chromosomes.
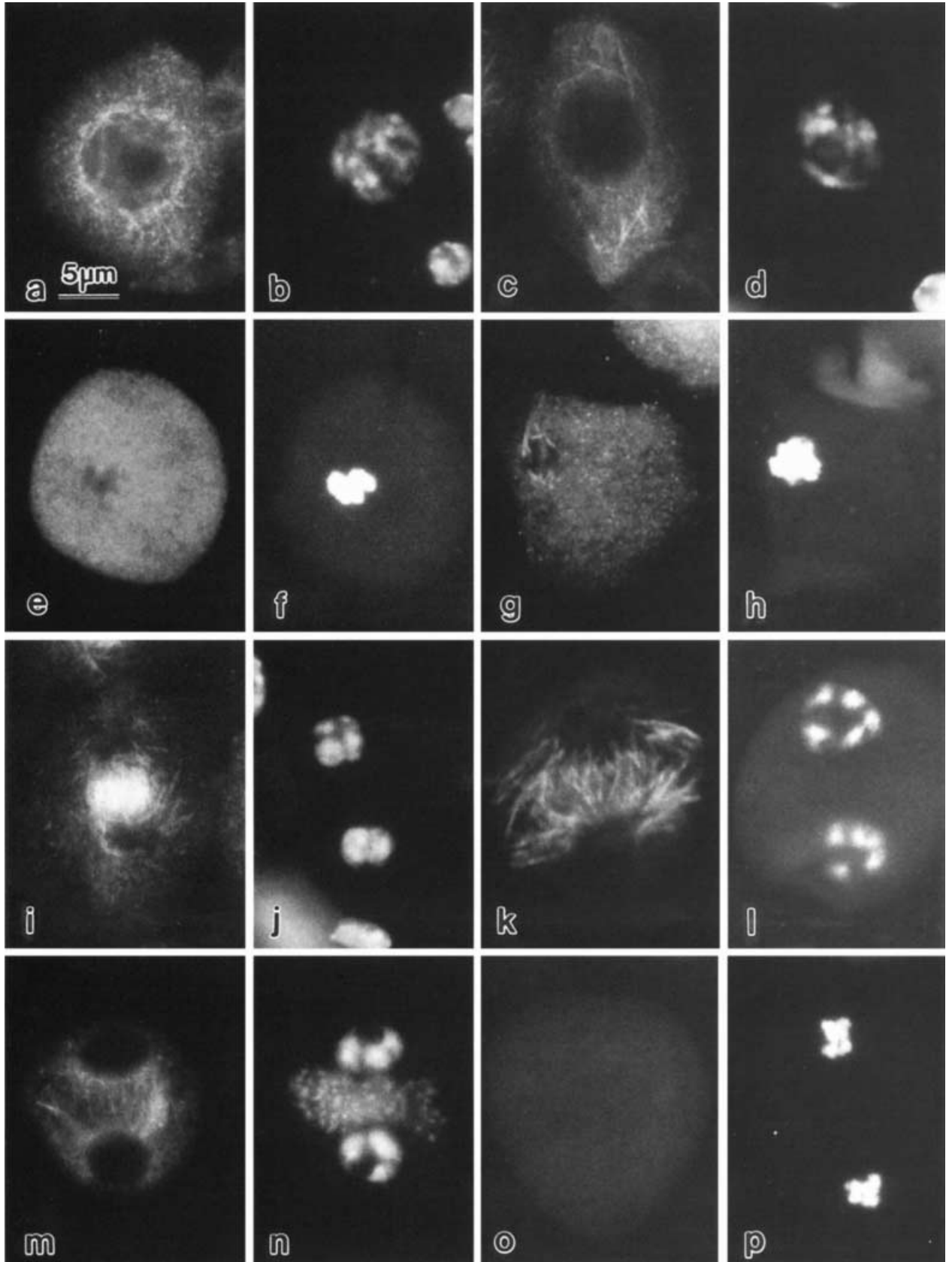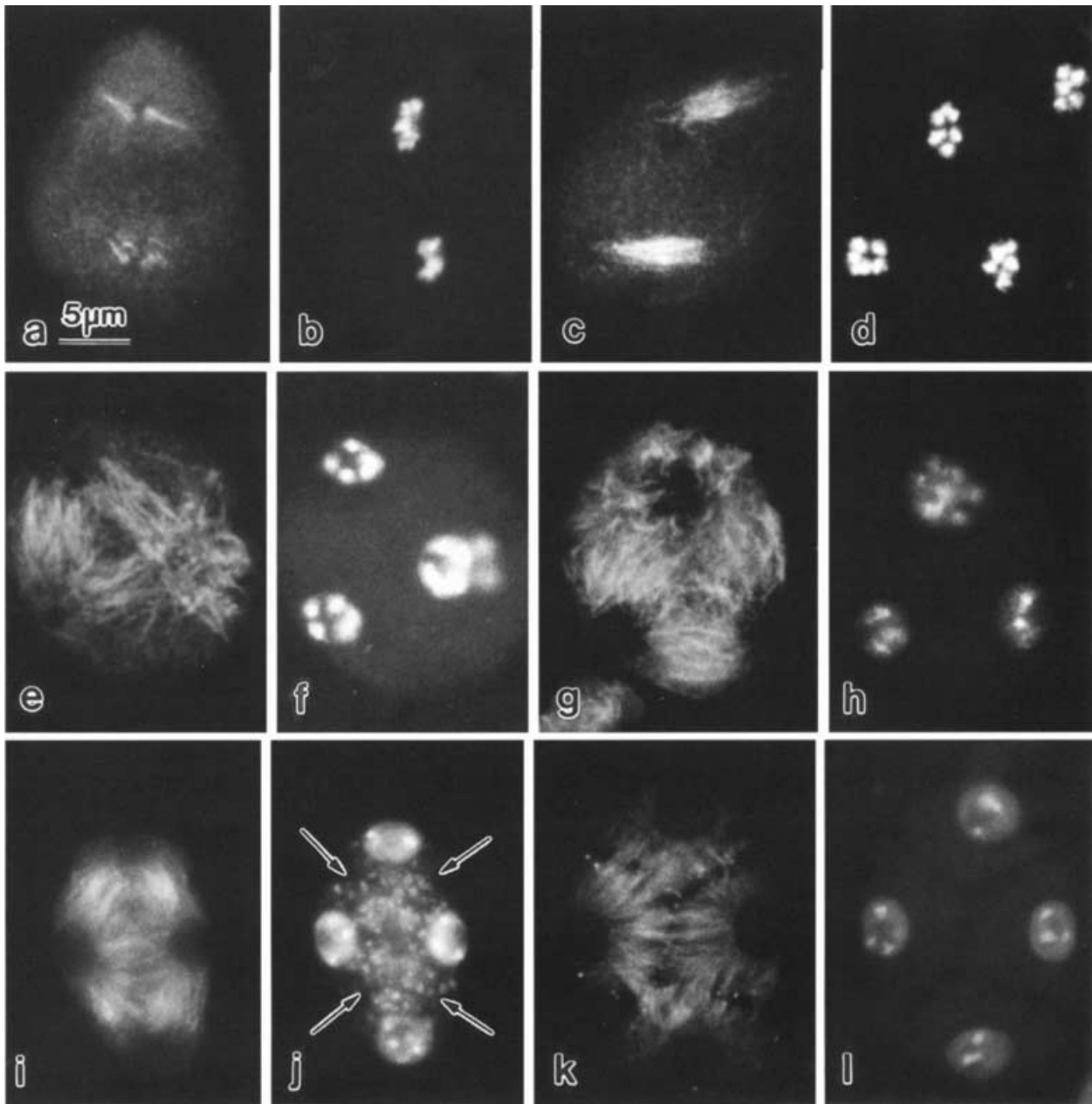
Figure 2. Fluorescence micrographs of meiosis in wild-type microsporocytes: metaphase II to cytokinesis.
(a, b) Metaphase II. (a) FITC. Spindle axes approximately parallel to equatorial plane. (b) Hoechst. Condensed and aligned chromosomes. (c, d) Telophase II. (c) FITC. Spindles with focused poles. (d) Hoechst. Five distinct chromosomes at each pole. (e, f) Early 'phragmoplast'. (e) FITC. Primary and secondary interzonal spindles between all four nuclei. (f) Hoechst. Individual chromosomes visible. (g, h) 'Phragmoplasts'. (g) FITC. MTs form a complex network of overlapping 'phragmoplasts'. (h) Hoechst. Chromosomes beginning to organize into nuclei. (i, j) Early cytokinesis. (i) FITC. MT arrays between all four nuclei. (j) Hoechst. Four nuclei with organelles throughout cytoplasm; early signs of infurrowing (arrows). (k, l) Late cytokinesis. (k) FITC. Only a few internuclear MTs remain. (l) Hoechst. Four haploid nuclei.

the spindle axes are approximately parallel to the equatorial plane (Figure 2a,b). However, the angle between the two spindle axes appears more variable, as some are parallel to each other (Figure 2a) and others are approximately perpendicular (not shown; one spindle would be positioned as shown in Figure 2a, the other would be rotated approximately 90° so that the poles are pointing into and out of the page). At telophase II, brightly fluorescing spindles and individual chromosomes are visible (Figure 2c,d). As the primary interzonal spindles broaden, secondary interzonal spindles form between non-sister nuclei until spindles between all four nuclei are equivalent (Figure 2e,f). Each MT array extends centrifugally to form a complex network of overlapping 'phragmoplasts' (Figure 2g,h). At this stage,

the chromosomes start to decondense, but there still appears to be close association between MTs and chromosomes, suggesting that nuclear envelopes have not completely formed (compare the jagged appearance of MTs at the poles in Figure 2g to the nuclear MT-free zones in Figure 1m). At the onset of cytokinesis, nuclear envelopes have re-formed and organellar DNA is again labeled (Figure 2i,j). At this stage, infurrowing of callose begins at the periphery of the coenocyte (arrows; evidenced by staining with aniline blue, data not shown). As cytokinesis proceeds, internuclear MT arrays are diminished and four callose-encased microspores are produced (Figure 2k,l).

Abnormal male meiosis in syn1

Preliminary analysis of microsporogenesis in *syn1* plants revealed 'tetrads' with five to eight microspores containing variable amounts of DNA, suggesting a defect in meiosis (Peirson *et al.*, 1996). The current cytological study shows that the first observable defect in *syn1* occurs at telophase I where chromosome segregation and microtubule arrangement are irregular. Subsequent developmental stages are affected, leading to complete male sterility.

Three general classes of telophase I were identified in inflorescences of *syn1*, all of which contain two main poles and DNA scattered throughout the cytoplasm; an example of each is shown in Figure 3. The first class (Figure 3a,b) has a spindle with a fluorescence intensity similar to that of WT early telophase I (Figure 1i). In this example, seven distinctly staining units can be seen at the lower pole (Figure 3b). Since they are smaller or more condensed than chromosomes at any WT stage, it is likely that each unit is a chromatid or a chromosome fragment, but they will hereafter be referred to as 'chromosomes' for the sake of simplicity.

An example of the second variation of telophase I in *syn1* plants is shown in Figure 3(c,d). Here a few distinct MTs extend between two main poles and shorter MTs extend to the equator (Figure 3c; compare to Figure 1k). Again, most of the DNA is highly condensed and located at the two poles, but some 'chromosomes' remain along the length of the spindle (Figure 3d).

The third class of telophase I cells observed in *syn1* (Figure 3e,f) is similar in some respects to WT late telophase I (Figure 1m,n): this class is observed much less frequently than the other two classes or stages of telophase I, the spindle contains a relatively small number of MTs, and organellar DNA is fluorescing. In *syn1*, however, nuclear envelopes are not apparent; 'chromosomes' are scattered throughout the cytoplasm and the organelles do not form a tight equatorial band.

Based on similarities to WT cells, it appears that these three classes of cells may represent successive stages corresponding to early, mid-, and late telophase I. However,

the variability observed in the spindle structures between the three classes may also be due in part to random segregation of chromosomes, i.e. variable chromosome segregation may lead to variable MT positioning, and the three classes may be comparable stages rather than sequential stages. Definitive assignment of the actual sequence of events is difficult because all three classes have been observed within a single locule, just as the three WT telophase I stages are observed within a single locule.

Defects that occur during meiosis I are propagated through the second meiotic division. The metaphase II spindles observed in *syn1* (Figure 3g) look almost identical to those in WT (Figure 2a), but 'chromosomes' are randomly distributed along the length of the spindle and are occasionally seen scattered throughout the cytoplasm (Figure 3h). The abnormal chromosome arrangement at metaphase leads to two varieties of altered telophase II; an example of each is shown in Figure 3. In the first (Figure 3i,j) the spindles look similar to WT (Figure 2c,d) but 'chromosomes' are again distributed along the entire length of the spindle and are scattered throughout the cytoplasm. A few stray MTs also appear independently of the two main spindles. In the second variation, spindles of various widths are present in the same cell, and DNA is distributed randomly among the spindles and the stray MTs (Figure 3k,l).

The next stage observed in *syn1* is similar to the WT early 'phragmoplast' stage in which MTs extend between all of the scattered 'chromosomes' (compare Figure 4a,b to Figure 2e,f). Each MT array then extends centrifugally to produce a complex cytoskeletal network; nuclear envelopes are formed around large and small groupings of 'chromosomes' (compare Figure 4c,d to Figure 2g,h). A later stage with micronuclei and fluorescing organelles is shown in Figure 4(e,f) (compare to Figure 2i,j). Cytokinesis occurs between most of the micronuclei to produce 'tetrads' with variable numbers and sizes of microspores, each containing a random amount of DNA (Figure 4g,h). Occasionally microspores are formed that contain two nuclei or micronuclei; electron microscopy reveals that each 'nucleus' is enclosed in a nuclear envelope (data not shown).

Discussion

While cytological studies of higher-plant male meiosis have provided a wealth of information regarding the physical changes associated with meiotic division (Brown and Lemmon, 1996 and references therein; Rhoades, 1950; Tanaka, 1991; Wolniak, 1976), very little is known about the proteins involved in this complex process. *A. thaliana* is being used as a model system for genetic and molecular studies on a number of aspects of cell growth and development (reviewed in Meyerowitz, 1989); with the modified cytological methods presented in this paper, it should also
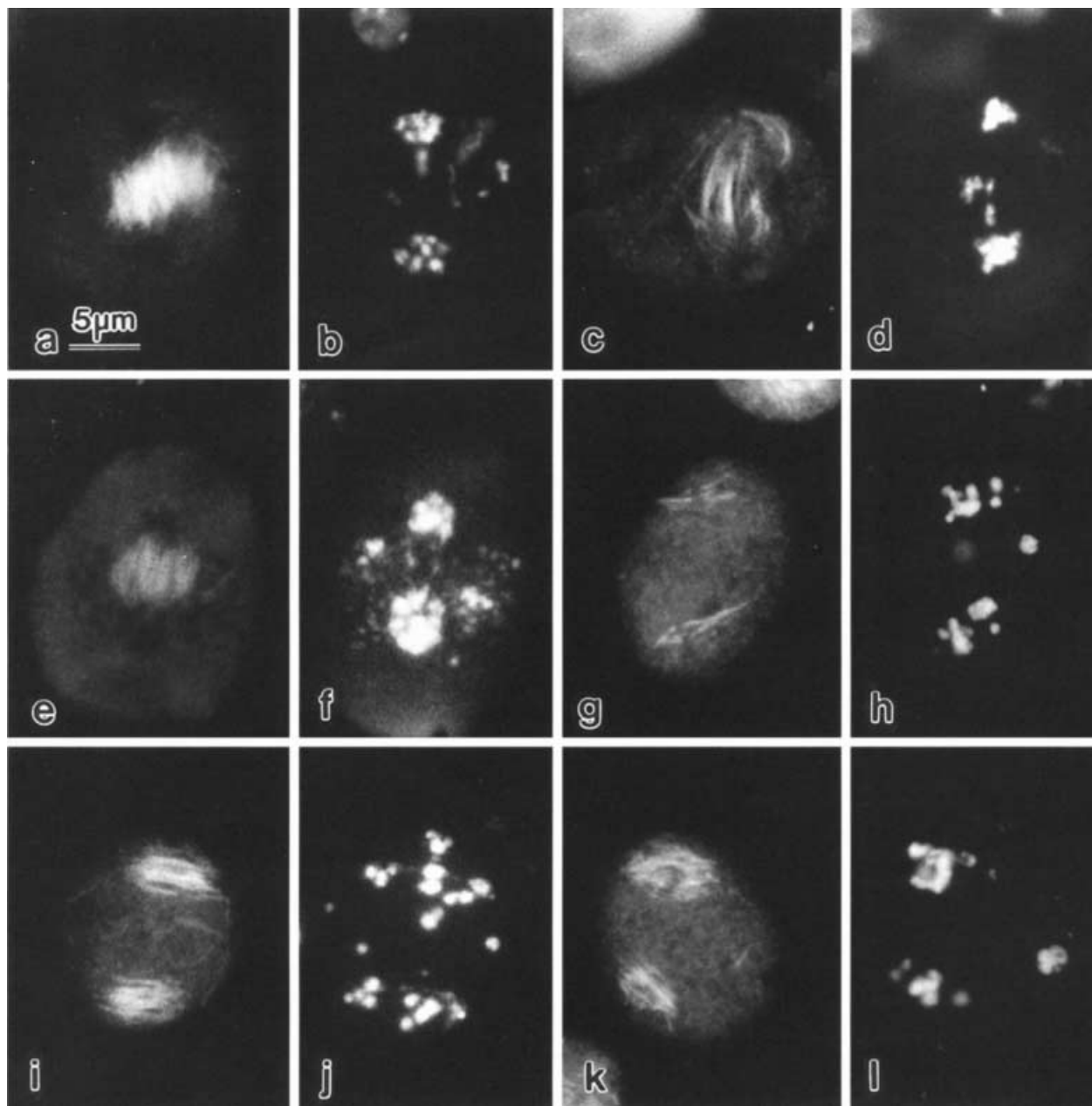
Figure 3. Fluorescence micrographs of abnormal meiosis in *syn1*: telophase I to telophase II.
(a, b) First variation of telophase I. (a) FITC. Brightly fluorescing spindle. (b) Hoechst. Seven distinct 'chromosomes' at lower pole; additional 'chromosomes' scattered throughout the cytoplasm. (c, d) Second variation of telophase I. (c) FITC. Distinct MTs between the two poles and extending from pole to equator. (d) Hoechst. Highly condensed DNA at two poles; some 'chromosomes' lagging along spindle. (e, f) Third variation of telophase I. (e) FITC. Lightly fluorescing spindle. (f) Hoechst. Majority of DNA at the poles; additional 'chromosomes' and organelles scattered throughout the cytoplasm. (g, h) Metaphase II. (g) FITC. Fairly normal-looking spindles. (h) Hoechst. 'Chromosomes' scattered along spindle and free in the cytoplasm. (i, j) First variation of telophase II. (i) FITC. Normal-looking spindles; stray MTs in the cytoplasm. (j) Hoechst. 'Chromosomes' scattered along spindle and free in the cytoplasm. (k, l) Second variation of telophase II. (k) FITC. Variable spindle widths; one stray MT. (l) Hoechst. Scattered 'chromosomes'.

become instrumental in the molecular characterization of meiotic genes.

Meiosis in wild-type A. thaliana *microsporocytes*

In order to provide a basis for the analysis of meiotic mutants, a detailed study of meiosis in WT *A. thaliana*

microsporocytes was conducted. While our results are generally consistent with observations in other angiosperms undergoing simultaneous cytokinesis (Brown and Lemmon, 1988; Hogan, 1987; Traas *et al.*, 1989; Van Lammeren *et al.*, 1985), two meiotic events were observed that have not been previously reported. These include (1) polarization of the microsporocyte cytoskeleton during
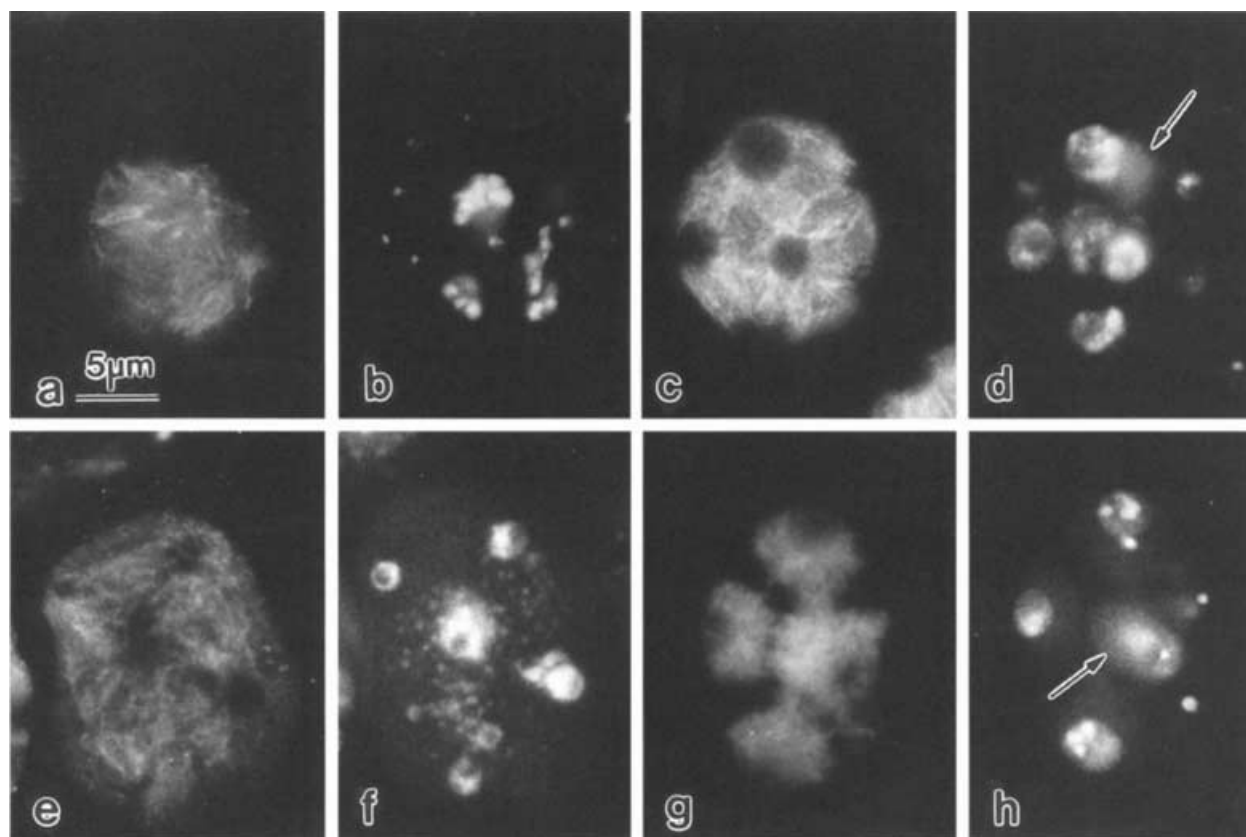
Figure 4. Fluorescence micrographs of abnormal meiosis in *syn1*: early 'phragmoplast' to cytokinesis.

(a, b) Early 'phragmoplast'. (a) FITC. MTs radiating in several directions from each nucleus. (b) Hoechst. Scattered 'chromosomes'. (c, d) 'Phragmoplasts.' (c) MTs radiate from each nucleus and form a complex network of overlapping 'phragmoplasts'. (d) Hoechst. Five nuclei/micronuclei and one small 'chromosome'. A sixth nucleus/micronucleus is out of the plane of focus (arrow). (e, f) Early cytokinesis. (e) FITC. Complex MT array. (f) At least seven nuclei/micronuclei with scattered organelles. (g, h) Late cytokinesis. (g) FITC. Only a few internuclear MT arrays remain. (h) Hoechst. Four nuclei/micronuclei and two small 'chromosomes'. A fifth nucleus is out of the plane of focus (arrow).

prophase I prior to nuclear envelope breakdown, and (2) extensive depolymerization of MTs just prior to metaphase II. The first observation could have implications regarding a previously uncharacterized mechanism for determining the axis of the metaphase I spindle. The second observation is peculiar since MTs are known to be involved in chromosome alignment in other species. Several lines of evidence indicate that these novel stages are real and not artifactual.

(1) Most of the meiotic figures presented here appear very similar to accepted stages of meiosis, indicating adequate fixation and specific antigen detection.

(2) The timing of the novel stages conforms to general patterns of chromosome condensation and cytoskeletal organization and was determined by observing developmentally ordered buds from more than 50 inflorescences.

(3) Stages with and without distinct spindles often appear on the same slide, indicating that the differences are stage-specific rather than a result of slight alterations in fixation or staining conditions.

In somatic cells, the axis of the metaphase spindle is determined by a pre-prophase band of MTs (reviewed in Wick, 1991). This equatorial MT array is perpendicular to the future metaphase spindle and encompasses the future cell division plane. However, no comparable structure has been documented in meiocytes. The only reported example of early division polarity in plant meiocytes is in maize, which undergoes successive cytokinesis. During late prophase I, each microsporocyte and its MT-encased nucleus elongate in the direction of the future spindle axis (Staiger and Cande, 1990). This elongation is also roughly parallel to the long axis of the anther. The authors suggest that the orientation and shape of the microsporocytes affect the position of the spindle axis and subsequently determine the locations of the division planes. However, most cytochemical studies of microsporocytes at prophase I reveal random cortical networks (Hogan, 1987; Traas *et al.*, 1989; Van Lammeren *et al.*, 1985), providing no clues to division polarity prior to establishment of the spindle.

The current study reveals a transition in prophase I cytoskeletal organization that may play a role in determin-

ing the axis of the metaphase I spindle in *A. thaliana* microsporocytes. As in previous studies of microsporogenesis (i.e. Staiger and Cande, 1990; Traas *et al.*, 1989; Van Lammeren *et al.*, 1985), early prophase I is characterized by an evenly distributed MT array along the surface of the nucleus. However, as chromatin condensation proceeds in *A. thaliana*, distinct MTs are observed at opposite ends of the microsporocyte, extending from the nuclear envelope to the cell wall. This cytoskeletal polarization may represent a previously uncharacterized mechanism for determining the axis of the metaphase I spindle during microsporogenesis. It also supports the concept that the nuclear envelope serves as a MT nucleating or organizing center in plant cells (Brown and Lemmon, 1996; Staiger and Cande, 1990). Additional studies are required to determine whether any other factors contribute to polarity in *A. thaliana* microsporocytes and whether such polarization occurs in other plant species.

The second meiotic event observed in WT *A. thaliana* that has not been reported in other angiosperms is the extensive depolymerization of MTs just prior to metaphase II. In many plant species, radial MT systems emanate from each telophase I nucleus and invade the nuclear region during or immediately following nuclear envelope breakdown (Brown and Lemmon, 1996; Hogan, 1987). This is followed by chromosome alignment and metaphase II spindle formation. Prometaphase MT arrays are observed in many other organisms and are likewise involved in chromosome orientation and spindle formation (reviewed in McKim and Hawley, 1995). In *A. thaliana* microsporocytes, however, very little β-tubulin staining is observed just prior to metaphase II, indicating the absence of a persistent radial MT system or prometaphase MT array. This stage has been observed in many *A. thaliana* inflorescences but its significance is not understood. Post-telophase I microfilament arrays have been observed in several plant species (Dinis and Mesquita, 1993; Traas *et al.*, 1989), but it is not yet known whether they affect chromosome alignment and metaphase II spindle orientation. Experiments are currently underway to localize actin in *A. thaliana* microsporocytes; the findings may provide additional insight into the role of the cytoskeleton in meiosis.

syn1

The T-DNA-tagged mutant *syn1* is the first *A. thaliana* meiotic mutant to be cytologically described. Although experiments are still in progress to isolate the gene involved in the mutation, this paper provides some insight into possible roles of the SYN1 protein.

The first observable defect in *syn1* is the presence of 'chromosomes' (i.e. chromosomes, chromatids, and/or chromosome fragments) that are not associated with the telophase I poles; MT distribution is also abnormal at this stage. During the second meiotic division, 'chromosomes' are dispersed along the entire length of the metaphase and telophase spindles. After nuclear division is complete, nuclear envelopes are formed around large and small groupings of DNA. All of the mutant microspores collapse soon after callose wall degradation, leading to complete male sterility. Female fertility is also affected; work is in progress to characterize meiosis during megasporogenesis in *syn1*.

The *syn1* phenotype is similar to those reported for synaptic mutants in a variety of plant species. Most of these studies involve chromosome staining and/or transmission electron microscopy (i.e. Golubovskaya, 1989; Johnston *et al.*, 1986; Kitada and Omura, 1983, 1984; Moens, 1969); MT organization has been described for only one synaptic mutant (*dsy**, Staiger and Cande, 1993). Synaptic mutants are characterized by the occurrence of unpaired chromosomes (univalents) as early as diakinesis. Univalents result when homologous chromosomes fail to pair at pachytene (asynapsis), or when initial pairing occurs but chromosomes dissociate prematurely so that the frequency of chiasmata formation is reduced (desynapsis). Since univalent chromosomes have only one centromere, they are unable to maintain the normal bipolar orientation along the metaphase I spindle; therefore, univalents move independently to the poles. The microspores produced by synaptic mutants are of various sizes and ploidy numbers, and normally do not develop into viable pollen grains. Most synaptic mutations also affect female fertility, suggesting that a set of genes controls homologous chromosome pairing and recombination in both anthers and ovules.

Because of the thin, tangled conformation of the chromosomes during synapsis, differentiation between asynaptic and desynaptic mutations is not always possible (Kaul and Murthy, 1985). *A. thaliana* microsporocytes are particularly difficult to analyze at this stage because of the small size of the chromosomes. However, two observations suggest that *syn1* could be classified as a desynaptic mutant: (1) the DNA aligns at the metaphase I plate, and (2) most of the DNA segregates into two main poles at telophase I. In most asynaptic mutants, the univalents are randomly scattered throughout the cytoplasm and never align at the equator. However, in a synaptic mutant of potato (*sy-2*), chromosome pairing was never observed, yet the univalents align at the metaphase I plate and segregate to two main poles (Johnston *et al.*, 1986). Since synaptonemal complex formation cannot be observed at this level of analysis, further studies are required (e.g. chromosome spreads or electron microscopy) in order to determine whether asynapsis or desynapsis occurs in *syn1*.

Although the mechanism that brings together homologous chromosomes at zygotene–pachytene is not completely understood, synaptonemal complex (SC) formation

certainly plays a role (reviewed in Moens, 1994). In fact, many synaptic mutants display abnormalities in the structure and function of the SC. In an asynaptic wheat mutant, lateral elements of the SC are normal but the central element required for binding the two homologs together appears to be absent (La Cour and Wells, 1970). The SC central region in a desynaptic maize mutant, *dsy1*, was found to be wider than normal and the connections between homologs are not as rigid as in WT cells (Maguire *et al.*, 1993). Three yeast genes have recently been cloned that encode structural components of the SC (*zip1*, *red1*, and *hop1*); mutations in these genes also result in abnormal synapsis (reviewed in Roeder, 1995).

Defects in synapsis not only result in recombination and chiasmata deficiencies, but may also hinder establishment of sister chromatid cohesion (reviewed in Bickel and Orr-Weaver, 1996). A desynaptic maize mutant, *dy1*, is deficient in chiasmata maintenance; the resulting univalents often undergo sister chromatid separation during anaphase I (Maguire, 1978). Abnormal chromosome segregation is also observed in a yeast mutant (*med1*; Rockmill and Roeder, 1994) and two *Drosophila* mutants (*mei-S332* and *ord*; reviewed in Orr-Weaver, 1995) that undergo precocious sister chromatid separation. The MEI-S332 protein localizes to the centromeric region of meiotic chromosomes from prophase I until sister chromatids separate in anaphase II (Kerrebrock *et al.*, 1995). The authors suggest that MEI-S332 maintains cohesion in the centromere regions of sister chromatids. The *Drosophila* ORD protein may maintain sister chromatid cohesion along the chromosome arms as well as at the centromere regions (Miyazaki and Orr-Weaver, 1992). In mutants with defects in sister chromatid cohesion, the number of individual DNA molecules observed at meiosis I is more than the diploid number of chromosomes, i.e. sister chromatids become detached from each other and remain as separate entities in the cytoplasm. This is similar to what is observed in *syn1* microsporocytes: $2n = 10$, but more than 10 distinctly staining units can be seen in each cell (i.e. Figure 3b), suggesting that *syn1* may be defective in sister chromatid cohesion.

The second meiotic division that occurs in *syn1* is similar to that observed in other synaptic mutants. Generally, the abnormalities observed in this division are consequences of the aberrant segregation that took place in the first division. Bipolar metaphase II spindles are formed and univalents presumably undergo normal separation of chromatids; additional chromatids or chromosome fragments are scattered throughout the cytoplasm. Almost all of the 'chromosomes' become nucleation sites for MT arrays and are organized into micronuclei. In general, the positioning of cleavage planes appears to be dependent on the location of the micronuclei, since most microspores contain only one nucleus or micronucleus. However, binucleate microspores are occasionally observed (confirmed by analysis of transmission electron micrographs, data not shown).

Because of the similarities between *syn1* and synaptic mutants from plants and other organisms, we propose that the SYN1 protein is involved in SC formation and/or cohesion between sister chromatids. Cloning of the *syn1* gene and additional *A. thaliana* meiotic genes should lead to exciting advances in our understanding of the meiotic process.

Experimental procedures

Plant material

Arabidopsis thaliana L. Heynh, ecotype Wassilewskija (WS) was the source of both WT and mutant plants. *syn1* was selected in a large-scale screen of T-DNA transformants at the DuPont Company, Wilmington, DE, USA (1990). Plants were maintained as previously described (Peirson *et al.*, 1996).

Fixation

In order to obtain the maximal number of meiotic figures, whole inflorescences were collected just prior to bolting (Vieira *et al.*, 1990) and pretreated with *m*-maleimidobenzoic acid *N*-hydroxysuccinimide ester (MBS) for 30 min at room temperature according to Sonobe and Shibaoka (1989), except that 50 mM potassium phosphate buffer, pH 8.0, was used (Nairn *et al.*, 1969). Inflorescences were then fixed for 1 h according to Wick (1993) in 3.7% (w/v) paraformaldehyde, 5 mM EGTA, 50 mM potassium phosphate buffer, but 5% (v/v) DMSO was added (Brown and Lemmon, 1991) and the pH was raised to 8.0. After three 10 min buffer rinses, the tissues were either stained immediately or stored in buffer for up to a month at 4°C.

Slide preparation and fluorescent staining

Anthers were dissected from 0.5–0.7 mm buds (Peirson *et al.*, 1996) and squashed between two poly-L-lysine (Sigma)-coated glass slides. The released sporogenous cells were immobilized with a thin layer of 0.94% (w/v) agarose, 0.94% (w/v) gelatin, 2.5% (w/v) glucose (modified from Clapham and Ostergren, 1984). Cells were then treated with 1.4% (w/v) β-glucuronidase, 7% (w/v) sucrose (aqueous) for 15 min at room temperature and rinsed with buffer (Clapham and Ostergren, 1984). Cells were subsequently incubated with 1% (v/v) Triton X-100 in buffer for 30 min, rinsed in buffer, and incubated overnight at 4°C with 100 μg ml⁻¹ mouse anti-β-tubulin (Developmental Studies Hybridoma Bank, Johns Hopkins University School of Medicine and the University of Iowa), 0.05% (v/v) Triton X-100 in antibody dilution buffer (0.02 M sodium phosphate, pH 8.0; 0.3 M NaCl; 0.1% (w/v) sodium azide; 4.5 mg ml⁻¹ BSA). Following buffer rinses, cells were treated for 6 h with 10 μg ml⁻¹ secondary antibody (FITC-conjugated F(ab) fragment goat anti-mouse IgG (Jackson ImmunoResearch Laboratories Inc., West Grove, PA), 0.05% (v/v) Triton X-100 in antibody dilution buffer). Slides were rinsed with buffer and the DNA was stained for 10 min with 0.01% (w/v) Hoechst 33258 in potassium phosphate buffer with 0.1% (v/v) Triton X-100 added (modified from Gantotti and Woodske, 1991). To decrease fading of the

fluorochrome, cover slips were mounted with 0.03% (w/v) *p*-phenylenediamine, 10% (v/v) glycerol in potassium phosphate buffer (Battaglia *et al.*, 1994), and slides were incubated for at least 20 min before viewing.

Photography

Microsporocytes were viewed and photographed with a Nikon Optiphot-2 equipped with epifluorescence. The objective used in this study was a Nikon CF N Plan 1000 × oil Achromat with iris, n.a. 1.25–0.5, and a 0.16 mm working distance. FITC-conjugated β-tubulin was observed with excitation filter 480/30, dichroic mirror 505 DCLP, barrier filter 535/40; stained DNA was viewed with excitation filter 360–420, dichroic mirror 420, barrier filter 450; and T-Max 400 film was used to capture the images.

Acknowledgments

References

Battaglia, M., Pozzi, D., Grimaldi, S. and Parasassi, T. (1994) Hoechst 33258 staining for detecting mycoplasma contamination in cell cultures: a method for reducing fluorescence photobleaching. *Biotech. Histochem.* **69**, 152–156.

Bickel, S.E. and Orr-Weaver, T.L. (1996) Holding chromatids together to ensure they go their separate ways. *BioEssays,* **18,** 293–300.

Brown, R.C. and Lemmon, B.E. (1988) Microtubules associated with simultaneous cytokinesis of coenocytic microsporocytes. *Am. J. Bot.* **75,** 1848–1856.

Brown, R.C. and Lemmon, B.E. (1991) Pollen development in orchids: 1. Cytoskeleton and the control of division plane in irregular patterns of cytokinesis. *Protoplasma,* **163,** 9–18.

Brown, R.C. and Lemmon, B.E. (1996) Nuclear cytoplasmic domains, microtubules and organelles in microsporocytes of the slipper orchid *Cypripedium californicum* A. Gray dividing by simultaneous cytokinesis. *Sex. Plant Reprod.* **9,** 145–152.

Chaudhury, A.M., Lavithis, M., Taylor, P.E., Craig, S., Singh, M.B., Signer, E.R., Knox, R.B. and Dennis, E.S. (1994) Genetic control of male fertility in *Arabidopsis thaliana*: structural analysis of premeiotic developmental mutants. *Sex. Plant Reprod.* **7,** 17–28.

Clapham, D.H. and Ostergren, G. (1984) Immunocytochemistry of tubulin at meiosis in *Tradescantia* by a protein-A gold method. *Hereditas,* **101,** 137–142.

Dawson, J., Wilson, Z.A., Aarts, M.G.M., Braithwaite, A.F., Briarty, L.G. and Mulligan, B.J. (1993) Microspore and pollen development in six male-sterile mutants of *Arabidopsis thaliana. Can. J. Bot.* **71,** 629–638.

Dinis, A.M. and Mesquita, J.F. (1993) The F-actin distribution during microsporogenesis in *Magnolia soulangeana* Soul. (Magnoliaceae). *Sex. Plant Reprod.* **6,** 57–63.

Gantotti, B.V. and Woodske, D.V.G. (1991) Nuclear staining of *Colletotrichum gloeosporiodes* F. Sp. *Malvae* conidia with fluorescent and nonfluorescent stains. *Biotech. Histochem.* **1,** 7–13.

Golubovskaya, I.N. (1989) Meiosis in maize: *mei* genes and conception of genetic control of meiosis. In *Advances in Genetics,* Volume 26 (Scandalios, J.G., ed.). San Diego: Academic Press, pp. 149–192.

He, C., Tirlapur, U., Cresti, M., Peja, M., Crone, D.E. and Mascarenhas, J.P. (1996) An *Arabidopsis* mutant showing aberrations in male meiosis. *Sex. Plant Reprod.* **9,** 54–57.

Hogan, C.J. (1987) Microtubule patterns during meiosis in two higher plant species. *Protoplasma* **138,** 126–136.

Johnston, S.A., Ruhde, R.W., Ehlenfeldt, M.K. and Hanneman, R.E. Jr. (1986) Inheritance and microsporogenesis of a synaptic mutant (*sy-2*) from *Solanum commersonii* Dun. *Can. J. Genet. Cytol.* **28,** 520–524.

Kaul, M.L.H. and Murthy, T.G.K. (1985) Mutant genes affecting higher plant meiosis. *Theor. Appl. Genet.* **70,** 449–466.

Kerrebrock, A.W., Moore, D.P., Wu, J.S. and Orr-Weaver, T.J. (1995) Mei-S332, a *Drosophila* protein required for sister-chromatid cohesion, can localize to meiotic centromere regions. *Cell,* **83,** 247–256.

Kitada, K. and Omura, T. (1983) Genetic control of meiosis in rice, *Oryza sativa* L. II. Cytogenetical analyses of desynaptic mutants. *Jpn J. Genet.* **58,** 567–577.

Kitada, K. and Omura, T. (1984) Genetic control of meiosis in rice, *Oryza sativa* L. IV. Cytogenetical analyses of asynaptic mutants. *Can. J. Genet. Cytol.* **26,** 264–271.

Kitada, K., Kurata, N., Satoh, H. and Omura, T. (1983) Genetic control of meiosis in rice, *Oryza sativa* L. I. Classification of meiotic mutants induced by MNU and their cytogenetical characteristics. *Jpn. J. Genet.* **58,** 231–240.

La Cour, L.F. and Wells, B. (1970) Meiotic prophase in anthers of asynaptic wheat: a light and electron microscopical study. *Chromosoma,* **29,** 419–427.

McKim, K.S. and Hawley, R.S. (1995) Chromosomal control of meiotic cell division. *Science,* **270,** 1595–1601.

Maguire, M.P. (1978) Evidence for separate genetic control of crossing over and chiasma maintenance in maize. *Chromosoma,* **65,** 173–183.

Maguire, M.P., Riess, R.W. and Paredes, A.M. (1993) Evidence from a maize desynaptic mutant points to a probable role of synaptonemal complex central region components in provision for subsequent chiasma maintenance. *Genome,* **36,** 797–807.

Meyerowitz, E.M. (1989) *Arabidopsis,* a useful weed. *Cell,* **56,** 263–269.

Miyazaki, W.Y. and Orr-Weaver, T.L. (1992) Sister-chromatid misbehavior in *Drosophila ord* mutants. *Genetics,* **132,** 1047–1061.

Moens, P.B. (1969) Genetic and cytological effects of three desynaptic genes in the tomato. *Can. J. Genet. Cytol.* **11,** 857–869.

Moens, P.B. (1994) Molecular perspectives of chromosome pairing at meiosis. *BioEssays,* **16,** 101–106.

Nairn R.C., Herzog, F., Ward, H.A. and De Boer, W.G.R.M. (1969) Microphotometry in immunofluorescence. *Clin. Exp. Immunol.* **4,** 697–705.

Orr-Weaver, T.L. (1995) Meiosis in *Drosophila*: seeing is believing. *Proc. Natl Acad. Sci. USA,* **92,** 10 443–10 449.

Peirson, B.N., Owen, H.A., Feldmann, K.A. and Makaroff, C.A. (1996) Characterization of three male-sterile mutants of *Arabidopsis thaliana* exhibiting alterations in meiosis. *Sex. Plant Reprod.* **9**, 1–16.

Rhoades, M.M. (1950) Meiosis in maize. *J. Hered.* **41**, 59–70.

Rockmill, B. and Roeder, G.S. (1994) The yeast *med1* mutant undergoes both meiotic homolog nondisjunction and precocious separation of sister chromatids. *Genetics,* **136**, 65–74.

Roeder, G.S. (1995) Sex and the single cell: meiosis in yeast. *Proc. Natl Acad. Sci. USA,* **92**, 10 450–10 456.

Sonobe, S. and Shibaoka, H. (1989) Cortical fine actin filaments in higher plant cells visualized by rhodamine–phalloidin after pretreatment with *m*-maleimidobenzoyl *N*-hydroxysuccinimide ester. *Protoplasma,* **148**, 80–86.

Staiger, C.J. and Cande, W.Z. (1990) Microtubule distribution in *dv*, a maize meiotic mutant defective in the prophase to metaphase transition. *Dev. Biol.* **138**, 231–242.

Staiger, C.J. and Cande, W.Z. (1993) Cytoskeletal analysis of maize meiotic mutants. In *Molecular and Cell Biology of the Plant Cell Cycle* (Ormrod, J.C. and Francis, D., eds). Dordrecht, The Netherlands: Kluwer Academic Publishers, pp. 157–171.

Tanaka, I. (1991) Microtubule-determined plastid distribution during microsporogenesis in *Lilium longiflorum. J. Cell Sci.* **99**, 21–31.

Traas, J.A., Burgain, S. and De Vaulx, R.D. (1989) The organization of the cytoskeleton during meiosis in eggplant (*Solanum melongena* (L.)): microtubules and F-actin are both necessary for coordinated meiotic division. *J. Cell Sci.* **92**, 541–550.

Van Lammeren, A.A.M., Keijzer, C.J., Willemse, M.T.M. and Kieft, H. (1985) Structure and function of the microtubular cytoskeleton during pollen development in *Gasteria verrucosa* (Mill.) H. Duval. *Planta,* **165**, 1–11.

Vieira, M.L.C., Briarty, L.G. and Mulligan, B.J. (1990) A method for analysis of meiosis in anthers of *Arabidopsis thaliana. Ann. Bot.* **66**, 717–719.

Wick, S.M. (1991) Spatial aspects of cytokinesis in plant cells. *Curr. Opin. Cell Biol.* **3**, 253–260.

Wick, S.M. (1993) Immunolabeling of antigens in plant cells. In *Methods in Cell Biology,* Volume 37 (Asai, D.J., ed.). San Diego: Academic Press, pp. 171–200.

Wolniak, S.M. (1976) Organelle distribution and apportionment during meiosis in the microsporocyte of *Ginkgo biloba* L. *Am. J. Bot.* **63**, 251–258.

Zetka, M.C. and Rose, A.M. (1995) Mutant *rec-1* eliminates the meiotic pattern of crossing over in *Caenorhabditis elegans. Genetics,* **141**, 1339–1349.